Inorganic Chemistry

Article

pubs.acs.org/IC

$(Nd_{1.5}Mg_{0.5})Ni_7$-Based Compounds: Structural and Hydrogen Storage Properties

Qingan Zhang,*[,†] Bin Zhao,[†] Miaohui Fang,[†] Chaoren Liu,[‡] Qingmiao Hu,[‡] Fang Fang,[§] Dalin Sun,[§] Liuzhang Ouyang,[∥] and Min Zhu*[,∥]

[†]School of Materials Science and Engineering, Anhui University of Technology, Maanshan 243002, China

[‡]Institute of Metal Research, Chinese Academy of Sciences, Shenyang 110016, China

[§]Department of Materials Science, Fudan University, Shanghai 200433, China

[∥]School of Materials Science and Engineering, South China University of Technology, Guangzhou 510641, China

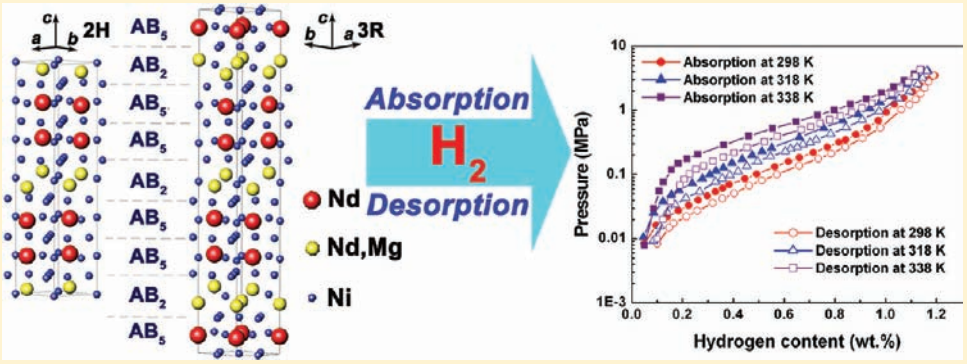

ABSTRACT: The structural and hydrogen storage properties of $(Nd_{1.5}Mg_{0.5})Ni_7$-based alloys (i.e., A_2B_7-type) with a coexistence of two structures (hexagonal 2H and rhombohedral 3R) are investigated in this study. In both 2H- and 3R-type A_2B_7 structures, Mg atoms occupy Nd sites of Laves-type AB_2 subunits rather than those of AB_5 subunits because Mg substitution for Nd in the AB_2 subunits more significantly strengthens the ionic bond in the system. An increase in the A-atomic radius or the B-atomic radius stabilizes the 2H structure, but a decrease in the A-atomic radius or the B-atomic radius is favorable for formation of the 3R structure. The 2H-A_2B_7 and 3R-A_2B_7 phases in each alloy have quite similar equilibrium pressures upon hydrogen absorption and desorption, which show a linear relationship with the average subunit volume. The hydriding enthalpy for the $(Nd_{1.5}Mg_{0.5})Ni_7$ compound is about −29.4 kJ/mol H_2 and becomes more negative with partial substitution of La for Nd and Co/Cu for Ni but less negative with partial substitution of Y for Nd.

INTRODUCTION

Since the use of La_2MgNi_9 and La_4MgNi_{19} compounds was reported as hydrogen storage materials,[1] ternary M−Mg−Ni (M = rare earth metals) compounds have been studied because their hydrogen storage properties are superior to corresponding binary M−Ni compounds.[2−20] Binary M−Ni compounds have layered structures where MNi_2 and MNi_5 subunits (also known as AB_2 and AB_5 subunits, respectively) stack along the c axis alternatively according to certain combinations.[21,22] In the ternary La_2MgNi_9 and La_4MgNi_{19} compounds, Mg atoms preferentially occupy some A sites in AB_2 subunits rather than AB_5 subunits,[7,15] which leads to superlattice structures with stacked AB_2 and AB_5 subunits. Although a similar phenomenon was also found in the $(La_{1.5}Mg_{0.5})Ni_7$ (i.e., the La_3MgNi_{14}) compound,[7] occupation of Mg atoms in $(M_{1.5}Mg_{0.5})Ni_7$ structures should be investigated systematically because there are two forms: viz., a hexagonal 2H structure (Ce_2Ni_7-type) and a rhombohedral 3R structure (Gd_2Co_7-type) in M_2Ni_7 compounds.[21] Moreover, for the Mg occupation in the $(M_{1.5}Mg_{0.5})Ni_7$ structures there is a lack of theoretical understanding. For this purpose, the $(Nd_{1.5}Mg_{0.5})Ni_7$ compound is selected in this research due to a coexistence of 2H and 3R forms in the binary Nd_2Ni_7 compound.[21] Site occupations of Mg atoms in 2H and 3R structures of $(Nd_{1.5}Mg_{0.5})Ni_7$ are investigated by Rietveld analysis of experimental X-ray powder diffraction (XRD) data and first-principles calculations based on density functional theory (DFT).

Furthermore, previous research revealed that the crystal structure of a binary M_2Ni_7 compound is size dependent; viz., the 2H structure is stable for larger M-atomic radii, the 3R structure is preferred for smaller M-atomic radii, and both structures coexist in the case of medium-sized M-atomic radii.[21] This phenomenon raises the question as to whether the crystal structure of ternary $(M_{1.5}Mg_{0.5})Ni_7$ compounds is also size dependent similar to binary M_2Ni_7 compounds. To clarify this question, the structural stabilities of 2H and 3R were studied by comparing their relative amounts in the $(Nd_{1.5}Mg_{0.5})Ni_7$-based compounds after partial substitution by different elements. On the basis of the

Received: October 24, 2011
Published: February 22, 2012

   dx.doi.org/10.1021/ic2022962 | *Inorg. Chem.* 2012, 51, 2976−2983

$(Nd_{1.5}Mg_{0.5})Ni_7$ compound, La and Y are used as larger and smaller substitutes for Nd, respectively, to change the average A-atomic radius. Similarly, Ni is partially replaced by Co or Cu to increase the average B-atomic radius because Ni has the smallest atomic radius among transition metals. Accordingly, correlations of the relative amounts of 2H-A_2B_7 and 3R-A_2B_7 phases with an average A-atomic radius or an average B-atomic radius are obtained to reveal structural stabilities.

From a hydrogen storage point of view, $(La_{1.5}Mg_{0.5})Ni_7$ with a 2H structure as a representative of $(M_{1.5}Mg_{0.5})Ni_7$ compounds can absorb and desorb hydrogen under moderate conditions.[23] Its hydride formation enthalpy is about −31.4 kJ/mol H_2, which is close to −30 kJ/mol H_2 for the $LaNi_5$−H_2 system.[24] However, hydrogen storage properties of $(Nd_{1.5}Mg_{0.5})Ni_7$ have not been reported to date. It is especially unclear whether $(Nd_{1.5}Mg_{0.5})Ni_7$ complies with the case of La_4MgNi_{19} that the two variants (2H and 3R phases) have almost the same thermodynamics of hydrogen absorption and desorption. Moreover, the effects of partial substitution for Nd or Ni in the $(Nd_{1.5}Mg_{0.5})Ni_7$ compound on the thermodynamics of hydrogen absorption and desorption also interest us because alloying is an effective method to improve hydrogen storage properties. Hence, the hydrogen absorption−desorption properties of $(Nd_{1.5}Mg_{0.5})Ni_7$-based compounds were finally investigated.

EXPERIMENTAL SECTION

Sample Preparation. $(Nd_{1.5}Mg_{0.5})Ni_7$, $(NdLa_{0.5}Mg_{0.5})Ni_7$, $(NdY_{0.5}Mg_{0.5})Ni_7$, $(Nd_{1.5}Mg_{0.5})(Ni_6Co)$, and $(Nd_{1.5}Mg_{0.5})(Ni_6Cu)$ alloys were prepared by the following steps: Appropriate amounts of pure metals were induction melted under an argon atmosphere (about 0.1 MPa). An excess of about 3 wt % of rare earth metals and 16 wt % of Mg was added to compensate for the losses of rare earth metals and Mg during melting. The as-obtained ingots were wrapped in tantalum foil and heated at 1273 K for 10 h under an argon atmosphere (1 MPa). The ingots were then cooled to 973 K, again held for 10 h, and finally quenched at room temperature.

Structural Characterization. Microstructural characteristics of $(Nd_{1.5}Mg_{0.5})Ni_7$-based alloys were examined using a scanning electron microscope (SEM) XL30 with an energy-dispersive X-ray spectrometer (EDX) at an accelerating voltage of 20 kV. Before SEM observation, the bulk samples were mechanically polished. To evaluate the phase structures, XRD measurements were carried out on a Rigaku D/Max 2500VL/PC diffractometer with Cu Kα radiation at 50 kV and 200 mA. XRD profiles were analyzed with the Rietveld refinement program RIETAN-2000.[25]

Calculation Method. Similar to a Ce_2Ni_7 structure,[21] the 2H-type Nd_2Ni_7 structure was modeled by a supercell containing 36 atoms where there are eight possible sites numbered 1−8 (see Figure 1a) and 10 possible site-occupation configurations as listed in Table 1 for Mg atoms in $(Nd_{1.5}Mg_{0.5})Ni_7$. On the basis of the Gd_2Ni_7 structure,[21] we employed a primitive cell containing 18 atoms for the 3R-type Nd_2Ni_7 structure where there are four possible sites numbered 1−4 (see Figure 1b) and two possible site-occupation configurations (see Table 1) for Mg atoms. The stable site occupancy of Mg atoms in both structures was determined by comparing the total energies of the systems with different site-occupation configurations. The total energies were calculated using the first-principles plane-wave pseudopotential method based on DFT which was implemented as a Vienna ab initio Simulation Package (VASP).[26−30] The projector-augmented wave (PAW) formalism,[31] an all-electron DFT technique with a computational efficiency close to pseudopotential techniques, was employed for the atomic potential. The exchange-correlation potential was described with the generalized gradient approximation (GGA) parametrized by Perdew and Wang.[32] The plane-wave cutoff energy was set as 360 eV. The k points were generated by the Monkhorst Pack scheme and sampled on grids of $6 \times 6 \times 2$ for 2H and $6 \times 6 \times 6$ for 3R. Integration over the Brillouin zone was performed by the improved tetrahedron method. Our test calculations demonstrated that the selected plane-wave cutoff energy and k-point mesh ensured an accuracy of about 0.3 meV for total energy calculations.

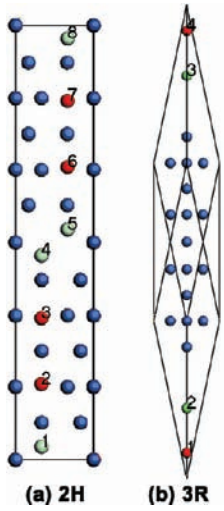

Figure 1. Possible sites for Mg atoms in (a) 2H- and (b) 3R-type Nd_2Ni_7 structures. Nd(1), Nd(2), and Ni sites are represented as green, red, and blue spheres, respectively.

Table 1. Total Energies (in eV/(36 atoms)) of $(Nd_{1.5}Mg_{0.5})Ni_7$ with Various Site-Occupation Configurations for Mg Atoms in both 2H- and 3R-type A_2B_7 Structures

	2H		3R	
	configuration	energy	configuration	energy
Nd_2Ni_7		−202.123		−202.136
Nd sites in $NdNi_2$ subunits	1, 4	−195.262	1, 4	−195.273
	1, 5	−195.274		
	1, 8	−194.894		
Nd sites in $NdNi_5$ subunits	2, 3	−192.825	2, 3	−193.011
	2, 6	−193.013		
	2, 7	−192.976		
mixing Nd sites in $NdNi_2$ and $NdNi_5$ subunits	1, 2	−193.883		
	1, 3	−194.107		
	1, 6	−194.147		
	1, 7	−194.103		

Hydrogen Absorption and Desorption. To investigate the hydrogen storage properties of $(Nd_{1.5}Mg_{0.5})Ni_7$-based compounds, pressure−composition (P−C) isotherms were measured using a Sieverts-type apparatus (Suzuki Shokan Co. Ltd., Japan) at 298, 318, and 338 K. The bulk samples were first ground to powders (less than 45 μm) in a glovebox under a dry argon atmosphere and then sealed in stainless steel containers. Prior to formal measurements, powder samples were heated in a vacuum at 423 K for 1 h and then activated by repeatedly hydriding−dehydriding at 353 K four times. During each cycle the samples were hydrided under a hydrogen pressure of 8 MPa for 1 h and subsequently dehydrided against a backpressure of 0.001 MPa for 1 h.

RESULTS AND DISCUSSION

Site Occupation of Mg. Figure 2a shows the Rietveld refinement of the XRD pattern of the $(Nd_{1.5}Mg_{0.5})Ni_7$ alloy with the coexistence of a hexagonal phase (2H-A_2B_7) and a rhombohedral phase (3R-A_2B_7) accompanied by minor impurity phases

dx.doi.org/10.1021/ic2022962 | Inorg. Chem. 2012, 51, 2976−2983

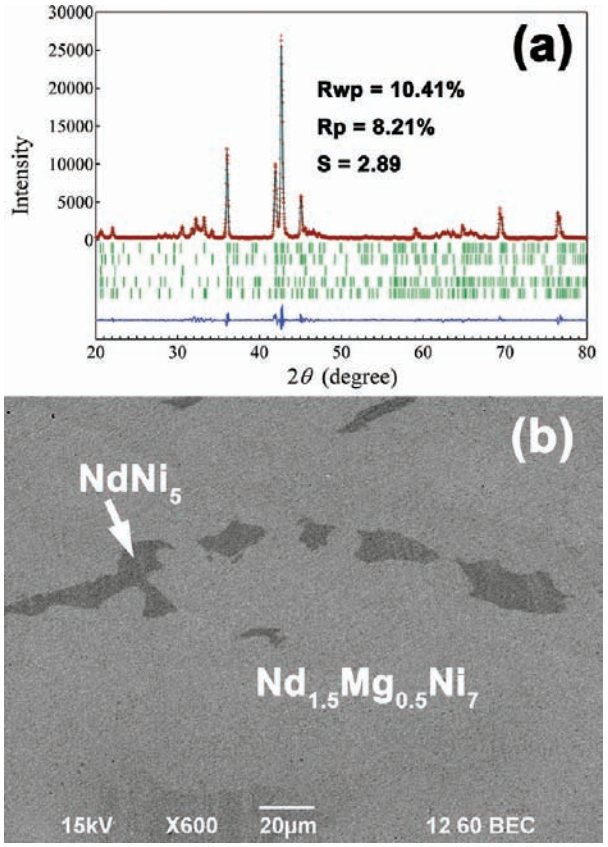

Figure 2. (a) Rietveld refinement of the observed XRD pattern and (b) backscattered SEM image of the $(Nd_{1.5}Mg_{0.5})Ni_7$ sample. Vertical bars below the patterns show the positions of all possible reflection peaks of the 2H-A_2B_7, 3R-A_2B_7, $NdNi_5$, 2H-A_5B_{19}, and 3R-A_5B_{19} phases.

$NdNi_5$, 2H-A_5B_{19}, and 3R-A_5B_{19}. For the Rietveld refinement, starting structure models for 2H-A_2B_7 and 3R-A_2B_7 phases were taken from reported data for $(La_{1.5}Mg_{0.5})Ni_7$ and $(Ca_{1.5}Mg_{0.5})Ni_7$,[7,19] respectively. Rietveld analysis revealed that the abundance of 2H-A_2B_7, 3R-A_2B_7, $NdNi_5$, 2H-A_5B_{19}, and 3R-A_5B_{19} phases are 35, 51, 5, 4, and 5 wt %, respectively. Compared with the binary Nd_2Ni_7 alloy consisting of 80 wt % of 2H-A_2B_7 phase and 20 wt % of 3R-A_2B_7 phase,[21] the present result suggests that partial substitution of Mg for Nd in Nd_2Ni_7 is favorable for formation of the 3R phase which agrees with our previous investigation on La_4MgNi_{19}.[20] Figure 2b shows the backscattered SEM image of the $(Nd_{1.5}Mg_{0.5})Ni_7$ alloy where the impurity phase $NdNi_5$ is clearly visible. However, 2H-A_2B_7 and 3R-A_2B_7 phases cannot be distinguished from each other under SEM due to their identical composition. Their average atomic composition was measured to be $Nd_{17.2\pm0.8}Mg_{5.8\pm0.5}Ni_{77.0\pm1.1}$, which is close to the nominal composition $Nd_{16.67}Mg_{5.55}Ni_{77.78}$. This result means that the influence of minor impurity phases on the composition of 2H-A_2B_7 and 3R-A_2B_7 phases can be neglected in this alloy.

Tables 2 and 3 list the refined atomic coordinates, isotropic thermal parameters, and occupation numbers for 2H- and 3R-type A_2B_7 structures in the $(Nd_{1.5}Mg_{0.5})Ni_7$ alloy, respectively. One-half of the Nd(1) sites are preferentially occupied by Mg atoms, but neither Nd(2) sites nor Ni sites are filled with Mg atoms in both 2H and 3R structures, which means that Mg atoms occupy the Nd sites in the Laves-type AB_2 subunits rather than the AB_5 subunit sites for both structures (see Figure 3).

Table 2. Atomic Coordinates, Isotropic Thermal Parameters (B Values), and Occupation Numbers (g Values) for the 2H-Type A_2B_7 Structure in the $(Nd_{1.5}Mg_{0.5})Ni_7$ Alloy Determined from XRD Data[a]

atom	site	g	x	y	z	B (nm^2)
Nd(1)/Mg(1)	4*f*	0.52(1)/0.48	1/3	2/3	0.0301(6)	0.011(2)
Nd(2)	4*f*	1.0	1/3	2/3	0.1743(4)	0.008(1)
Ni(1)	2*a*	1.0	0	0	0	0.012(2)
Ni(2)	4*e*	1.0	0	0	0.1680(5)	0.010(1)
Ni(3)	4*f*	1.0	1/3	2/3	0.8325(6)	0.009(1)
Ni(4)	6*h*	1.0	0.8378(6)	2*x*	1/4	0.009(2)
Ni(5)	12*k*	1.0	0.8358(5)	2*x*	0.0858(7)	0.010(2)

[a]Space group $P6_3/mmc$ (no. 194). Cell parameters: a = 0.49775(3) nm and c = 2.4098(4) nm.

Table 3. Atomic Coordinates, Isotropic Thermal Parameters (B Values), and Occupation Numbers (g Values) for the 3R-Type A_2B_7 Structure in the $(Nd_{1.5}Mg_{0.5})Ni_7$ Alloy Determined from XRD Data[a]

atom	site	g	x	y	z	B (nm^2)
Nd(1)/Mg(1)	6*c*	0.51(1)/0.49	0	0	0.1492(2)	0.016(2)
Nd(2)	6*c*	1.0	0	0	0.0546(5)	0.002(1)
Ni(1)	3*b*	1.0	0	0	1/2	0.011(1)
Ni(2)	6*c*	1.0	0	0	0.2782(4)	0.010(1)
Ni(3)	6*c*	1.0	0	0	0.3881(5)	0.010(1)
Ni(4)	9*e*	1.0	1/2	0	0	0.009(1)
Ni(5)	18*h*	1.0	0.4972(3)	−*x*	0.1090(4)	0.009(1)

[a]Space group $R\bar{3}m$ (no. 166). Cell parameters: a = 0.49780(6) nm and c = 3.6187(7) nm.

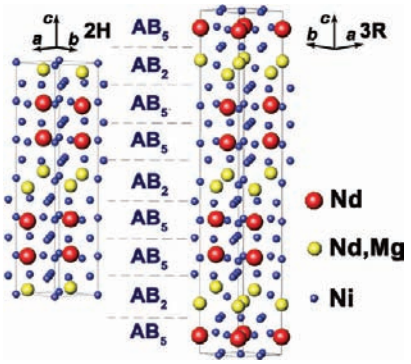

Figure 3. Structure stacking models for 2H- and 3R-type $(Nd_{1.5}Mg_{0.5})Ni_7$. Nd, (Nd+Mg), and Ni atoms are represented as red, yellow, and blue spheres, respectively.

This preferential occupation of Mg atoms in $(Nd_{1.5}Mg_{0.5})Ni_7$ structures is identical to ternary La_2MgNi_9 and La_4MgNi_{19} compounds,[7,15] which is favorable for hydrogen absorption−desorption properties.[19,20]

To fully understand the reason for the preferential site occupation of Mg in Nd_2Ni_7 as determined by XRD measurements, we calculated the total energies of $(Nd_{1.5}Mg_{0.5})Ni_7$ with different site-occupation configurations of Mg atoms as listed in Table 1. For the 2H-type A_2B_7 structure, there are 10 different possible site-occupation configurations for two Mg atoms in the supercell (see Figure 1a). Our calculations show that configurations with Nd1−Nd4 and Nd1−Nd5 sites (corresponding to the Nd(1) site in Table 2) are almost energetically degenerated and lower in

dx.doi.org/10.1021/ic2022962 | Inorg. Chem. 2012, 51, 2976−2983

energy (and therefore, more stable) than the other eight configurations. Note that Nd1, Nd4, and Nd5 belong to AB_2 subunits, and therefore, Mg atoms prefer to occupy Nd sites in AB_2 subunits, which is in agreement with the XRD measurement. For the 3R-type A_2B_7 structure, there are only two possible site-occupation configurations since the calculations are performed with the primitive cell containing only one Mg atom. We found that the Nd1−Nd4 configuration (corresponding to the Nd(1) site in Table 3 in AB_2 subunits is 2.262 eV/(36 atoms) lower in energy and therefore more stable than the Nd2−Nd3 configuration (corresponding to the Nd(2) site in Table 3) in AB_5 subunits and again is in agreement with XRD measurement.

Table 4. Electron Transfer in Undoped and Mg-Doped 2H-Type Nd_2Ni_7 Compounds[a]

subunit	atom	undoped	Mg in $NdNi_2$ subunit	Mg in $NdNi_5$ subunit
$NdNi_2$	Nd/*Mg*	−1.151	*−1.466*	−1.162
	Ni1	+0.512	+0.584	+0.505
	Ni2	+0.416	+0.517	+0.411
$NdNi_5$	Nd/*Mg*	−1.381	−1.388	*−1.519*
	Ni1	+0.416	+0.421	+0.403
	Ni2	+0.278	+0.279	+0.256
	Ni3	+0.285	+0.276	+0.277
	Ni4	+0.312	+0.294	+0.352
	Ni5	+0.284	+0.288	+0.348

[a]Positive values indicate electron gains, negative values indicate electron losses, and values of electron losses of the Mg atoms are shown in italic font.

For both Nd_2Ni_7 and $Nd_{1.5}Mg_{0.5}Ni_7$ with the stable site occupation of Mg, the total energy difference (<0.4 meV) between 2H- and 3R-type A_2B_7 structures approaches the accuracy of first-principles calculations which indicates that 2H- and 3R-type A_2B_7 structures are almost equally stable and further explains the coexistence of 2H and 3R phases in Nd_2Ni_7 and $Nd_{1.5}Mg_{0.5}Ni_7$.

To explore the physics underlying the site occupancy of Mg in Nd_2Ni_7, we analyzed the bonding character in the 2H-type $(Nd_{1.5}Mg_{0.5})Ni_7$ with different site occupations of Mg atoms. Using the Bader charge analysis technique,[33−35] we found significant electron transfer from Nd/Mg to Ni in this system (see Table 4), which indicates that the bonds in the $(Nd_{1.5}Mg_{0.5})Ni_7$ compound are somehow ionic in nature. For the binary Nd_2Ni_7, the Nd of the AB_2 subunit loses about 1.151 electrons while the Nd of the AB_5 subunit loses about 1.381 electrons in the 2H-type A_2B_7 structure. The Mg atom replacing the Nd atom in the AB_2

Table 5. Bond Length (in nm) between Nd/Mg and Its Surrounding Ni in Undoped and Mg-Doped 2H-type Nd_2Ni_7 Compounds[a]

subunit	bond	undoped	Mg in $NdNi_2$ subunit	Mg in $NdNi_5$ subunit
$NdNi_2$	Nd/*Mg*−Ni1	0.2870	*0.2807*	0.2818
	Nd/*Mg*−Ni2	0.2983	*0.2958*	0.2985
$NdNi_5$	Nd/*Mg*−Ni1	0.3290	0.3200	*0.3289*
	Nd/*Mg*−Ni2	0.2896	0.2874	*0.2877*
	Nd/*Mg*−Ni3	0.2896	0.2874	*0.2876*
	Nd/*Mg*−Ni4	0.3113	0.3172	*0.3019*

[a]Bond lengths associated with Mg are shown in italic font.

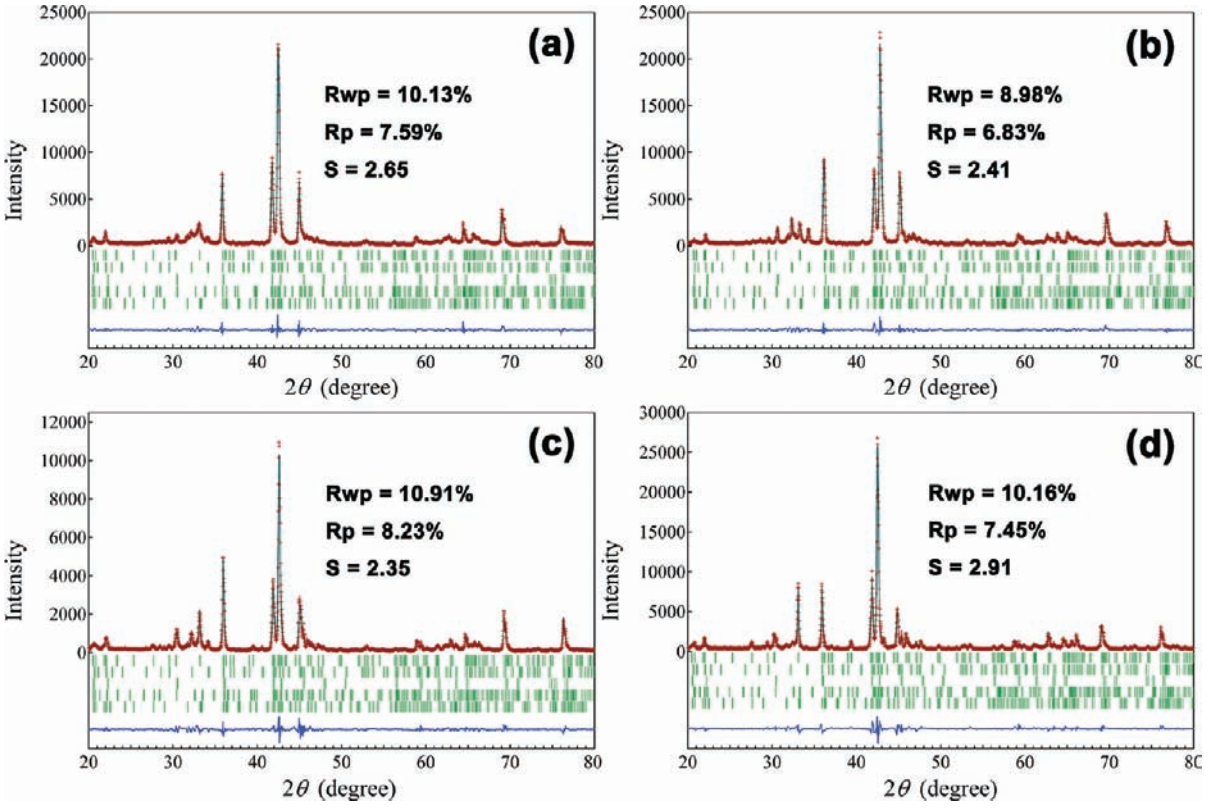

Figure 4. Rietveld refinements of observed XRD patterns for the (a) $(NdLa_{0.5}Mg_{0.5})Ni_7$, (b) $(NdY_{0.5}Mg_{0.5})Ni_7$, (c) $(Nd_{1.5}Mg_{0.5})(Ni_6Co)$, and (d) $(Nd_{1.5}Mg_{0.5})(Ni_6Cu)$ samples. Vertical bars below the patterns show the positions of all possible reflection peaks of the 2H-A_2B_7, 3R-A_2B_7, $NdNi_5$, 2H-A_5B_{19}, and 3R-A_5B_{19} phases.

dx.doi.org/10.1021/ic2022962 | *Inorg. Chem.* 2012, 51, 2976−2983

Table 6. Lattice Parameters and Abundance of Each Phase in $(Nd_{1.5}Mg_{0.5})Ni_7$-Based Alloys Determined from XRD Data[a]

compound	phases	lattice parameters (nm) a	lattice parameters (nm) c	abundance (wt %)
$(Nd_{1.5}Mg_{0.5})Ni_7$	2H-A_2B_7	0.49773(4)	2.4098(6)	35
		0.4978	2.4033	
	3R-A_2B_7	0.49784(7)	3.6187(7)	51
		0.4983	3.6062	
	$NdNi_5$	0.49683(5)	0.3977(9)	5
	2H-A_5B_{19}	0.49740(5)	3.1942(8)	4
	3R-A_5B_{19}	0.49776(8)	4.8202(5)	5
$(NdLa_{0.5}Mg_{0.5})Ni_7$	2H-A_2B_7	0.49978(7)	2.4155(7)	42
		0.4995	2.4069	
	3R-A_2B_7	0.49979(4)	3.6236(6)	45
		0.4987	3.6097	
	$NdNi_5$	0.49881(8)	0.3979(7)	6
	2H-A_5B_{19}	0.50009(7)	3.1974(8)	3
	3R-A_5B_{19}	0.49916(9)	4.8312(6)	4
$(NdY_{0.5}Mg_{0.5})Ni_7$	2H-A_2B_7	0.49588(1)	2.4058(8)	22
		0.4963	2.3934	
	3R-A_2B_7	0.49593(7)	3.6088(1)	63
		0.4960	3.5901	
	$NdNi_5$	0.49412(2)	0.3975(5)	9
	2H-A_5B_{19}	0.49604(6)	3.1902(8)	2
	3R-A_5B_{19}	0.49576(8)	4.8145(9)	4
$(Nd_{1.5}Mg_{0.5})(Ni_6Co)$	2H-A_2B_7	0.49849(6)	2.4166(8)	53
	3R-A_2B_7	0.49841(6)	3.6153(4)	35
	$NdNi_5$	0.49715(6)	0.3986(9)	7
	2H-A_5B_{19}	0.49823(7)	3.2080(6)	2
	3R-A_5B_{19}	0.49839(7)	4.8253(8)	3
$(Nd_{1.5}Mg_{0.5})(Ni_6Cu)$	2H-A_2B_7	0.49953(3)	2.4234(5)	78
	3R-A_2B_7	0.49907(5)	3.6221(5)	10
	$NdNi_5$	0.49807(6)	0.3991(3)	6
	2H-A_5B_{19}	0.49840(7)	3.2278(8)	3
	3R-A_5B_{19}	0.49959(8)	4.8372(7)	3

[a]Lattice parameters without standard deviation were obtained from first-principles calculations.

subunit loses about 1.466 electrons, whereas the Mg atom replacing the Nd atom in the AB_5 subunit loses about 1.519 electrons; both amounts are greater than the electron losses of the host Nd atoms, which means that substitution of Nd in either the AB_2 or the AB_5 subunit by Mg increases the ionic bond strength. On the other hand, the Mg−Ni bonds in $(Nd_{1.5}Mg_{0.5})Ni_7$ are shorter in length than the Nd−Ni bonds in Nd_2Ni_7 (see Table 5), which further enhances ionic bonds in the system. Although Mg substitution strengthens ionic bonds in both AB_2 and AB_5 units, the net electron increment induced by Mg substitution of Nd in AB_2 subunits (0.31) is more than twice the amount induced by Mg substitution of Nd in the AB_5 subunit (0.14). Accordingly, the strengthening of the ionic bond by Mg substitution of Nd in the AB_2 subunit is expected to be more significant than Mg substitution of Nd in the AB_5 subunit, which makes the former more stable than the latter. Therefore, Mg atoms prefer to occupy Nd sites in AB_2 subunits instead of AB_5 subunits sites.

Effect of Atomic Size. Figure 4a and 4b shows Rietveld refinements of XRD patterns for $(NdLa_{0.5}Mg_{0.5})Ni_7$ and $(NdY_{0.5}Mg_{0.5})Ni_7$ alloys, respectively. The abundance of each phase in the alloys was obtained by Rietveld refinements (see Table 6). Partial substitution of La for Nd leads to an increase in the relative amount of the 2H-A_2B_7 phase from 35 to 42 wt % but a decrease in the relative amount of the 3R-A_2B_7 phase from 51 to 45 wt %. On the contrary, the amount of the 2H-A_2B_7 phase decreases to 22 wt % while the amount of the 3R-A_2B_7 phase increases to 63 wt % when Nd is partially substituted by Y. Because the atomic radius of Nd is smaller than the atomic radius of La but larger than the atomic radius of Y, the average A-atomic radius increases or decreases due to partial substitution of La or Y for Nd. Hence, this result suggests that the increase in the A-atomic radius is favorable for formation of the 2H-A_2B_7 phase in ternary $(M_{1.5}Mg_{0.5})Ni_7$ alloys (see Figure 5a),

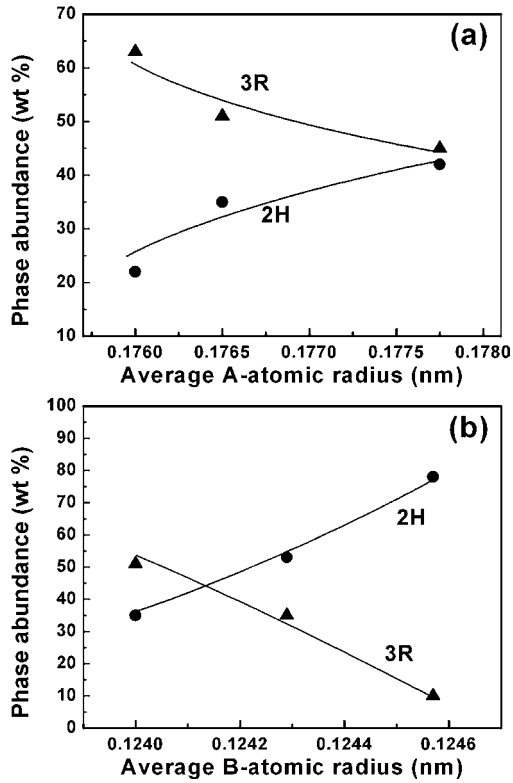

Figure 5. Correlations of the phase abundance of 2H-A_2B_7 and 3R-A_2B_7 phases with (a) average A-atomic radius and (b) average B-atomic radius, respectively, in A_2B_7-type alloys.

which complies with the binary M_2Ni_7 compounds whose layered structure is size dependent;[21] i.e., with the preference of a 2H structure for larger A-atomic radii and the 3R structure for smaller A-atomic radii.

To our knowledge, the influence of the B-atomic radius on the crystal structure in A_2B_7 compounds is unclear. To clarify this question, XRD patterns for $(Nd_{1.5}Mg_{0.5})(Ni_6Co)$ and $(Nd_{1.5}Mg_{0.5})(Ni_6Cu)$ were also refined (see Figure 4c and 4d, respectively). The abundance of each phase listed in Table 6 indicates that partial substitution of Co or Cu for Ni leads to an increase in the 2H-A_2B_7 phase and a decrease in the 3R-A_2B_7 phase. Figure 5b displays the correlation of the phase abundance of 2H-A_2B_7 and 3R-A_2B_7 phases with an average B-atomic radius in A_2B_7-type compounds, which

dx.doi.org/10.1021/ic2022962 | Inorg. Chem. 2012, 51, 2976−2983

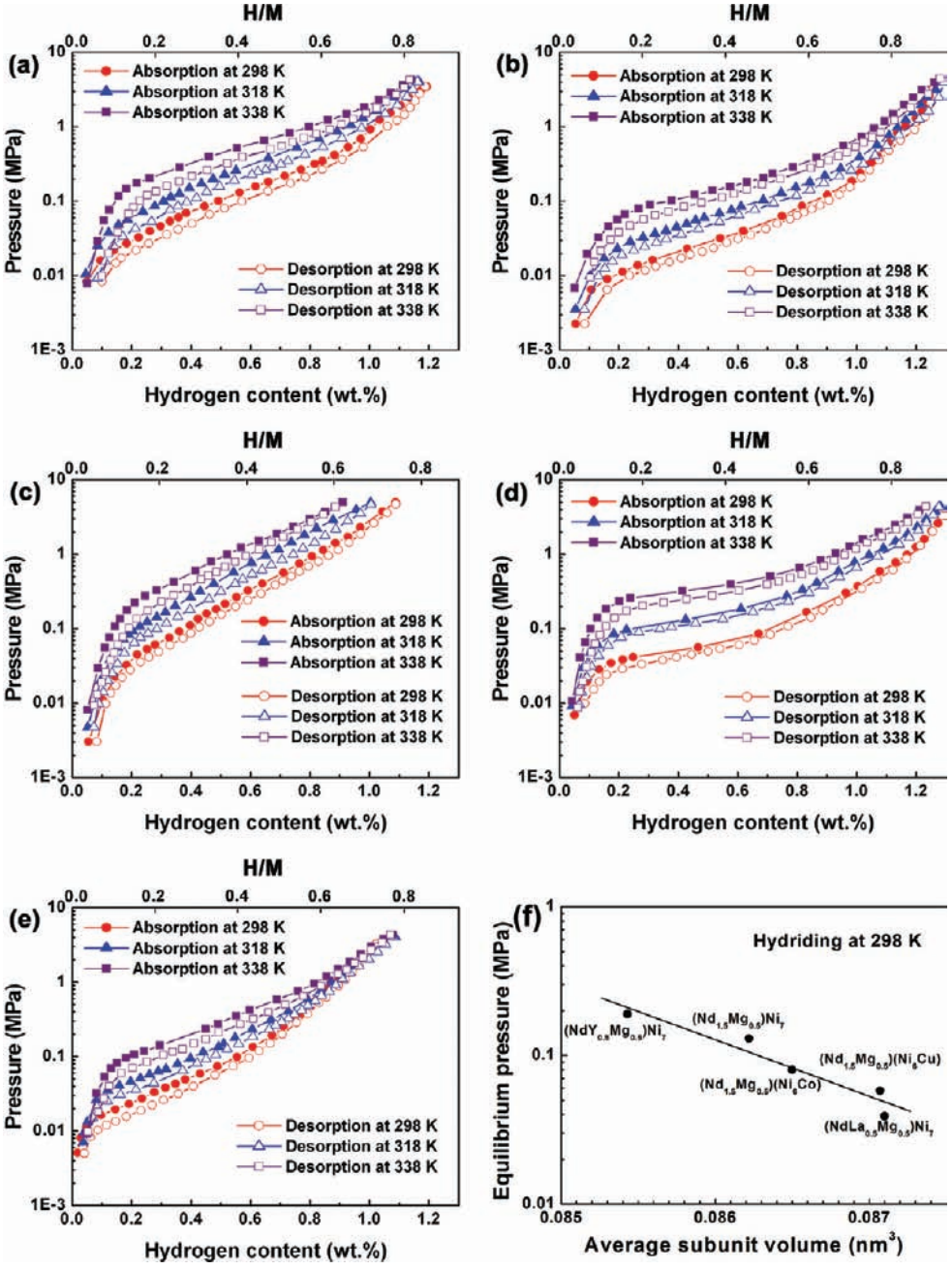

Figure 6. *P*−*C* isotherms of hydrogen absorption and desorption for (a) $(Nd_{1.5}Mg_{0.5})Ni_7$, (b) $(NdLa_{0.5}Mg_{0.5})Ni_7$, (c) $(NdY_{0.5}Mg_{0.5})Ni_7$, (d) $(Nd_{1.5}Mg_{0.5})(Ni_6Co)$, and (e) $(Nd_{1.5}Mg_{0.5})(Ni_6Cu)$ samples. (f) Correlation of the equilibrium pressure in the hydriding process at 298 K with an average subunit volume of the 2H and 3R phases in the A_2B_7-type alloys.

clearly shows that a larger B-atomic radius is also favorable for formation of the 2H-A_2B_7 phase.

Furthermore, the lattice parameters of 2H-A_2B_7 and 3R-A_2B_7 phases in the $(Nd_{1.5}Mg_{0.5})Ni_7$-based alloys obtained from XRD patterns are also listed in Table 6, which indicates that partial substitution of Nd or Ni by an element with a larger atomic radius leads to lattice expansion of both structures and vice versa. These changes in lattice parameters are confirmed by first-principles calculations (see Table 6), although lattice parameters for $(Nd_{1.5}Mg_{0.5})(Ni_6Co)$ and $(Nd_{1.5}Mg_{0.5})(Ni_6Cu)$ were not calculated due to a much higher computational complexity. Such a lattice expansion or contraction significantly influences hydrogen absorption−desorption properties which will be discussed below.

Hydrogen Storage. Pressure−composition isotherms (*P*−*C* isotherms) of the $(Nd_{1.5}Mg_{0.5})Ni_7$ alloy measured at 298, 318, and 338 K are shown in Figure 6a, where the following two features are observable. (i) Only one plateau is visible on each curve at each temperature, which suggests that the 2H-A_2B_7 and 3R-A_2B_7 phases have quite similar equilibrium pressures upon hydrogen absorption and desorption, although the plateau shows a large sloping characteristic similar to 2H-type $(La_{1.5}Mg_{0.5})Ni_7$.[23] (ii) The hydrogen absorption capacity of $(Nd_{1.5}Mg_{0.5})Ni_7$ is about 1.2 wt % (i.e., the atom ratio of hydrogen to metal H/M = 0.87) at 298 K, which is slightly smaller than the value of 1.4 wt % (H/M = 1) for $(La_{1.5}Mg_{0.5})Ni_7$.[23] However, hydrogen desorption shows good reversibility and small hysteresis due to preferential occupation of Mg in AB_2 subunits of $(Nd_{1.5}Mg_{0.5})Ni_7$.

dx.doi.org/10.1021/ic2022962 | *Inorg. Chem.* 2012, 51, 2976−2983

Figure 6b, 6c, 6d, and 6e shows $P-C$ isotherms of the $(NdLa_{0.5}Mg_{0.5})Ni_7$, $(NdY_{0.5}Mg_{0.5})Ni_7$, $(Nd_{1.5}Mg_{0.5})(Ni_6Co)$, and $(Nd_{1.5}Mg_{0.5})(Ni_6Cu)$ alloys, respectively. Compared with the results of $(Nd_{1.5}Mg_{0.5})Ni_7$, the following changes can be observed. (i) Partial substitution of La for Nd or Co for Ni leads to a flattening of the sloping plateau, whereas partial substitution of Y for Nd or Cu for Ni increases the plateau slope and reduces the total hydrogen capacity. However, there seems to be no simple relationship between sloping plateau behavior and the atomic size of a substitute. The degree of sloping is generally considered to be related to compositional inhomogeneity.[36,37] Hence, the sloping characteristic of $(Nd_{1.5}Mg_{0.5})Ni_7$-based compounds (whether A-site substitution or B-site substitution) can be improved by a long-time annealing. (ii) By taking the equilibrium pressures from the midpoints of sloping plateaus for $P-C$ isotherms, partial substitution of Y for Nd increases the equilibrium pressure of hydrogen, but partial substitution of La for Nd, Co for Ni, or Cu for Ni decreases the equilibrium pressure. The changes in equilibrium pressure caused by these substitutions are generally attributed to changes in lattice parameters (see Table 6) due to different atomic radii of substitutes. In this study, use of the average subunit volume instead of the unit cell volume is more reasonable for a correlation with equilibrium pressure due to the coexistence of 2H and 3R phases. Figure 6f represents the relationship of the equilibrium pressure in the hydriding process at 298 K with the average subunit volume of 2H and 3R phases of A_2B_7-type compounds. A linear relationship between equilibrium pressure and average subunit volume is obtained which can be used for practical selection of the type of substitution in development of new A_2B_7-type compounds.

The van't Hoff plots for $A_2B_7-H_2$ systems are displayed in Figure 7. For each system, the enthalpy changes of 2H-A_2B_7 and 3R-A_2B_7 phases are averaged and listed in Table 7 because of their close equilibrium pressures. Hydriding enthalpies for $(Nd_{1.5}Mg_{0.5})Ni_7$-based compounds range from −28.5 to −32.6 kJ/mol H_2, which further confirms that hydride formation enthalpies for ternary M−Mg−Ni compounds are close to −30 kJ/mol H_2 for the $LaNi_5-H_2$ system.[24,38] Nevertheless, the influence of partial substitution on the hydriding enthalpy is dimly visible in this study. For A-site substitution, the hydriding enthalpy decreases from −29.4 to −32.6 kJ/mol H_2 when Nd is partially replaced by La but increases to −28.5 kJ/mol H_2 due to partial substitution of Y for Nd. This result compares favorably with previous research on formation of hydrides from the $R_{0.2}La_{0.8}Ni_5$ (R = La, Y, and Nd) compounds,[39] which implies that occupation of hydrogen atoms in AB_5 subunits of $(NdLa_{0.5}Mg_{0.5})Ni_7$ and $(NdY_{0.5}Mg_{0.5})Ni_7$ compounds may be dominant during formation of hydrides. For B-site substitution, partial substitution of Co for Ni leads to an increase in the absolute value of hydriding enthalpy, which is consistent with results for the $LaNi_4Co$ compound.[39] Similarly, the increase in the absolute value of the hydriding enthalpy for $(Nd_{1.5}Mg_{0.5})(Ni_6Cu)$ also compares with the reported result that partial replacement of Ni by Cu stabilizes the $LaNi_5$ hydride.[39,40] Evidently, the effects of partial substitution for Nd or Ni on the thermodynamics of hydrogen absorption and desorption of the $(Nd_{1.5}Mg_{0.5})Ni_7$ compound comply with those of $LaNi_5$-based alloys.[38−41]

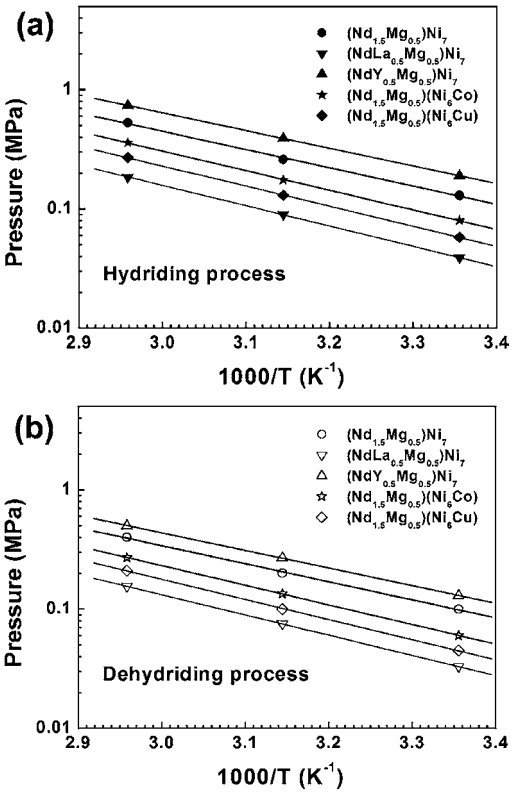

Figure 7. van't Hoff plots for the $A_2B_7-H_2$ systems in (a) hydriding and (b) dehydriding processes.

Table 7. Hydriding and Dehydriding Properties for $A_2B_7-H_2$ Systems

	hydriding		dehydriding	
system	enthalpy (kJ/mol H_2)	entropy (J/K mol H_2)	enthalpy (kJ/mol H_2)	entropy (J/K mol H_2)
$(Nd_{1.5}Mg_{0.5})Ni_7-H_2$	−29.4	−100.7	29.0	97.2
$(NdLa_{0.5}Mg_{0.5})Ni_7-H_2$	−32.6	−102.6	32.4	100.5
$(NdY_{0.5}Mg_{0.5})Ni_7-H_2$	−28.5	−100.9	28.2	96.9
$(Nd_{1.5}Mg_{0.5})(Ni_6Co)-H_2$	−31.5	−102.8	31.4	101.2
$(Nd_{1.5}Mg_{0.5})(Ni_6Cu)-H_2$	−32.2	−103.2	32.3	101.3

CONCLUSIONS

A systematic investigation of the structural and hydrogen storage properties of $(Nd_{1.5}Mg_{0.5})Ni_7$-based compounds was conducted in the this study. The $(Nd_{1.5}Mg_{0.5})Ni_7$ alloy is composed of a hexagonal phase (2H-A_2B_7) and a rhombohedral phase (3R-A_2B_7) accompanied by minor impurity phases $NdNi_5$, 2H-A_5B_{19}, and 3R-A_5B_{19}. In the 2H- and 3R-type A_2B_7 structures, Mg atoms occupy Nd sites of Laves-type AB_2 subunits rather than the Nd sites of the AB_5 subunits as demonstrated by both XRD measurements and first-principles calculations because Mg substitution of the Nd in the AB_2 subunits more significantly strengthens the ionic bond in the system. Furthermore, the phase abundance of $(Nd_{1.5}Mg_{0.5})Ni_7$, $(NdLa_{0.5}Mg_{0.5})Ni_7$, $(NdY_{0.5}Mg_{0.5})Ni_7$, $(Nd_{1.5}Mg_{0.5})(Ni_6Co)$, and $(Nd_{1.5}Mg_{0.5})(Ni_6Cu)$ alloys indicates that an increase in the A-atomic radius or the B-atomic radius stabilizes the 2H structure, but a decrease in the A-atomic radius or the B-atomic radius is favorable for formation of the 3R structure. The 2H-A_2B_7 and 3R-A_2B_7 phases in each compound have quite similar equilibrium pressures for hydrogen absorption and desorption, which show a linear relationship with the average subunit volume. The hydriding enthalpy for the $(Nd_{1.5}Mg_{0.5})Ni_7$ compound is about −29.4 kJ/mol H_2, which becomes more negative because of the partial substitutions of La for Nd and Co/Cu for Ni but less negative due to partial substitution of Y for Nd.

dx.doi.org/10.1021/ic2022962 | Inorg. Chem. 2012, 51, 2976−2983

AUTHOR INFORMATION

Corresponding Author

*E-mail: zhang03jp@yahoo.com.cn (Q.Z.); memzhu@scut.edu.cn (M.Z.).

Notes

The authors declare no competing financial interest.

ACKNOWLEDGMENTS

This work was financially supported by the National Basic Research Program of China (no. 2010CB631302) and the National Natural Science Foundation of China (nos. 50971001, 50871114, and 50925102).

REFERENCES

(1) Kadir, K.; Sakai, T.; Uehara, I. *J. Alloys Compd.* **1997**, *257*, 115−121.
(2) Kadir, K.; Kuriyama, N.; Sakai, T.; Uehara, I.; Eriksson, L. *J. Alloys Compd.* **1999**, *284*, 145−154.
(3) Kohno, T.; Yoshida, H.; Kawashima, F.; Inaba, T.; Sakai, I.; Yamamoto, M.; Kanda, M. *J. Alloys Compd.* **2000**, *311*, L5−L7.
(4) Iwase, K.; Sakaki, K.; Nakamura, Y.; Akiba, E. *Inorg. Chem.* **2010**, *49*, 8763−8768.
(5) Iwase, K.; Sakaki, K.; Matsuda, J.; Nakamura, Y.; Ishigaki, T.; Akiba, E. *Inorg. Chem.* **2011**, *50*, 4548−4552.
(6) Iwase, K.; Mori, K.; Hoshikawa, A.; Ishigaki, T. *Inorg. Chem.* **2011**, 50 DOI: 10.1021/ic201569m.
(7) Hayakawa, H.; Akiba, E.; Gotoh, M.; Kohno, T. *Mater. Trans.* **2005**, *46*, 1393−1401.
(8) Ozaki, T.; Kanemoto, M.; Kakeya, T.; Kitano, Y.; Kuzuhara, M.; Watada, M.; Tanase, S.; Sakai, T. *J. Alloys Compd.* **2007**, *446/447*, 620−624.
(9) Chai, Y. J.; Sakaki, K.; Asano, K.; Enoki, H.; Akiba, E.; Kohno, T. *Scr. Mater.* **2007**, *57*, 545−548.
(10) Zhang, J.; Fang, F.; Zheng, S.; Zhu, J.; Chen, G.; Sun, D.; Latroche, M.; Percheron-Guégan, A. *J. Power Sources* **2007**, *172*, 446−450.
(11) Escobar, D.; Srinivasan, S.; Goswami, Y.; Stefanakos, E. *J. Alloys Compd.* **2008**, *458*, 223−230.
(12) Zhang, J.; Zhou, G.; Chen, G.; Latroche, M.; Percheron-Guégan, A.; Sun, D. *Acta Mater.* **2008**, *56*, 5388−5394.
(13) Miraglia, S.; Girard, G.; Fruchart, D.; Liang, G.; Huot, J.; Schulz, R. *J. Alloys Compd.* **2009**, *478*, L33−L36.
(14) Chai, Y.; Asano, K.; Sakaki, K.; Enoki, H.; Akiba, E. *J. Alloys Compd.* **2009**, *485*, 174−180.
(15) Ferey, A.; Cuevas, F.; Latroche, M.; Knosp, B.; Bernard, P. *Electrochim. Acta* **2009**, *54*, 1710−1714.
(16) Nakamura, J.; Iwase, K.; Hayakawa, H.; Nakamura, Y.; Akiba, E. *J. Phys. Chem. C* **2009**, *113*, 5853−5859.
(17) Si, T. Z.; Pang, G.; Zhang, Q. A.; Liu, D. M.; Liu, N. *Int. J. Hydrogen Energy* **2009**, *34*, 4833−4837.
(18) Si, T. Z.; Zhang, Q. A.; Pang, G.; Liu, D. M.; Liu, N. *Int. J. Hydrogen Energy* **2009**, *34*, 1483−1488.
(19) Zhang, Q. A.; Pang, G.; Si, T. Z.; Liu, D. M. *Acta Mater.* **2009**, *57*, 2002−2009.
(20) Zhang, Q. A.; Fang, M. H.; Si, T. Z.; Fang, F.; Sun, D. L.; Ouyang, L. Z.; Zhu, M. *J. Phys. Chem. C* **2010**, *114*, 11686−11692.
(21) Buschow, K. H. J.; van Der Goot, A. S. *J. Less-Common Met.* **1970**, *22*, 419−428.
(22) Yamamoto, T.; Inui, H.; Yamaguchi, M.; Sato, K.; Fujitani, S.; Yonezu, I.; Nishio, K. *Acta Mater.* **1997**, *45*, 5213−5221.
(23) Denys, R. V.; Riabov, A. B.; Yartys, V. A.; Sato, M.; Delaplane, R. G. *J. Solid State Chem.* **2008**, *181*, 812−821.
(24) van Vucht, J. H. N.; Kuijpers, F. A.; Bruning, H. C. A. M. *Philips Res. Rep.* **1970**, *25*, 133−140.
(25) Izumi, F.; Ikeda, T. *Mater. Sci. Forum* **2000**, *321/323*, 198−203.
(26) Dreizler, R. M.; Gross, E. K. U. *Density Functional Theory*; Springer: Berlin, 1998.
(27) Kresse, G.; Furthmuller. *J. Comput. Mater. Sci.* **1996**, *6*, 15−50.
(28) Kresse, G.; Furthmüller. *J. Phys. Rev. B* **1996**, *54*, 11169.
(29) Kresse, G.; Hafner. *J. Phys. Rev. B* **1993**, *47*, 558.
(30) Kresse, G.; Hafner. *J. Phys. Rev. B* **1994**, *49*, 14251.
(31) Blochl, P. E. *Phys. Rev. B* **1994**, *50*, 17953.
(32) Perdew, J, P.; Wang, Y. *Phys. Rev. B* **1992**, *46*, 12947.
(33) Tang, W.; Sanville, E.; Henkelman, G. *J. Phys.: Condens. Matter* **2009**, *21*, 084204.
(34) Sanville, E.; Kenny, S. D.; Smith, R.; Henkelman, G. *J. Comput. Chem.* **2007**, *28*, 899−908.
(35) Henkelman, G.; Arnaldsson, A.; Josson, H. *Comput. Mater. Sci.* **2006**, *36*, 254−360.
(36) Luo, S.; Park, C. N.; Flanagan, T. B. *J. Alloys Compd.* **2004**, *384*, 208−216.
(37) Ledovskikh, A.; Danilov, D.; Notten, P. H. L. *Phys. Rew. B* **2007**, *76*, 064106.
(38) Shilov, A. L.; Kost, M. E.; Kuznetsov, N. T. *J. Less-Common Met.* **1988**, *144*, 23−30.
(39) Van Mal, H. H.; Buschow, K. H. J.; Miedema, A. R. *J. Less-Common Met.* **1974**, *35*, 65−76.
(40) Veremeeva, O. A.; Yakovleva, N. A.; Klyamkin, S. N.; Berdonosova, E. A.; Shelekhov, E. V. *Russ. Chem. Bull. (Int. Ed.)* **2006**, *55*, 949−954.
(41) Osumi, Y.; Suzuki, H.; Kato, A.; Oguro, K.; Nakane, M. *J. Less-Common Met.* **1980**, *74*, 271−277.